



1 **INFLUENCE OF LATE QUATERNARY CLIMATE ON THE BIOGEOGRAPHY OF**
2 **NEOTROPICAL AQUATIC SPECIES AS REFLECTED BY NON-MARINE**
3 **OSTRACODES**
4

5 Sergio Cohuo^{1,2}, Laura Macario-González^{1,3}, Sebastian Wagner⁴, Katrin Naumann¹,
6 Paula Echeverria¹; Liseth Pérez¹, Jason Curtis⁵; Mark Brenner⁵, Antje Schwalb¹

7
8 ¹Institut für Geosysteme und Bioindikation, Technische Universität Braunschweig,
9 Langer Kamp 19c, 38106 Braunschweig, Germany

10 ²Tecnológico Nacional de México/I. T. Chetumal. Av. Insurgentes 330, Chetumal,
11 77013 Quintana Roo, México

12 ³Tecnológico Nacional de México/I. T. de la Zona Maya. Carretera Chetumal-
13 Escárcega Km 21.5, ejido Juan Sarabia, 77965 Quintana Roo, México.

14 ⁴Helmholtz-Zentrum Geesthacht, Zentrum für Material- und Küstenforschung.
15 Max-Planck-Straße 1, 21502 Geesthacht, Germany

16 ⁵Department of Geological Sciences, and Land Use and Environmental Change
17 Institute, University of Florida, Gainesville, Florida, 32611, USA

18
19

20 **Abstract**
21

22 We evaluated how ranges of four endemic and non-endemic aquatic ostracode
23 species changed in response to long-term (glacial-interglacial cycles) and abrupt
24 climate fluctuations during the last 155 ka in the northern Neotropical region. We
25 employed two complementary approaches, fossil records and species distribution
26 modeling (SDM). Fossil assemblages were obtained from sediment cores PI-1, PI-2,
27 PI-6 and Petén-Itzá 22-VIII-99 from Petén Itzá Scientific Drilling Project, Lake Petén
28 Itzá, Guatemala. To obtain a spatially resolved pattern of (past) species distribution, a
29 downscaling cascade is employed. SDM's were reconstructed for the Last Interglacial
30 (~120 ka BP), the Last Glacial Maximum (~22 ka BP) and the middle Holocene (~6 ka
31 BP). During glacial/interglacial cycles and Marine Isotope Stages, modeled paleo-
32 distributions and paleo-records show nearly continuous presence of endemic and
33 non-endemic species in the region, suggesting negligible effects of long-term climate
34 variations on aquatic niche stability. During periods of abrupt ecological disruption
35 such as Heinrich Stadial 1 (HS1), endemic species were resilient, remaining within
36 their current areas of distribution. Non-endemic species, however, proved to be more
37 sensitive. Modeled paleo-distributions suggest that the geographic range of non-
38 endemic species changed, moving southward into Central America. Due to the
39 uncertainties involved in the downscaling from the global numerical to the highly



40 resolved regional geospatial statistical modelling, results can be seen as benchmark
41 for future studies using similar approaches. Given relatively moderate temperature
42 decreases in Lake Petén Itzá waters (~5°C) and persistence of some aquatic
43 ecosystems even during periods of severe drying in HS1, our data suggest 1)
44 existence of micro-refugia and/or 2) continuous interaction between central
45 metapopulations and surrounding populations, enabling aquatic taxa to survive
46 climate fluctuations in the northern Neotropical region.

47

48 **Keywords:** Climate change, freshwater ostracodes, Neotropics, fossil records,
49 species niche modelling.

50

51 **1 Introduction**

52 Climate changes are quasi-cyclical natural processes that continuously influence
53 ecosystem dynamics and shape biological diversity worldwide. During the Late
54 Quaternary, climate fluctuations such as glacial/Interglacial cycles, are recognized as
55 the main drivers responsible for past species extinctions (Martínez-Meyer et al.,
56 2004; Nogués-Bravo et al., 2008), speciation events (Peterson and Nyári, 2008;
57 Solomon et al., 2008), delimitation of refugia (Hugall et al., 2002; Peterson et al.,
58 2004) and development of migration pathways (Ruegg et al., 2006; Waltari and
59 Guralnick, 2009) for both plants and animals. In the northern Neotropics, which
60 include southern Mexico, Central America and the Antilles, late Quaternary climate
61 inferences based on climatic simulations with global climate models (GCMs)
62 (Hijmans et al., 2005) and reconstructions from marine and lacustrine sedimentary
63 sequences (Hodell et al., 2008; Pérez et al., 2011,2013; Escobar et al., 2012) have
64 revealed climate fluctuations related to temperature and precipitation, especially
65 during transitions between glacial and interglacial episodes, and during climate
66 pulses such as the Last Glacial Maximum (LGM) and Heinrich stadials (HS) (Correa-
67 Metrio et al., 2012b). In the Neotropics, controls of climate fluctuations are related to
68 orbital forcing and internal component variations, such as the position (north-south) of
69 the inter tropical convergence zone (ITCZ), strength of Atlantic meridional overturning
70 circulation (AMOC) and changes in Caribbean surface water temperature (Cohuo et
71 al., 2018). Alterations in these features have produced temperature decreases in a



72 range of 3 -5°C, although some estimations suggest decreases up to 10°C relative to
73 present and large reductions in precipitation, particularly during HS, when most lakes
74 in the region dried completely (Cohuo et al., 2018). Correa-Metrio et al. (2014) found
75 evidence for rapid climate change in terrestrial environments during HS, which was
76 associated with major ecological and biological shifts (Loarie et al., 2009; Burrows et
77 al., 2011; Sandel et al., 2011). Correa-Metrio et al. (2012a, b, 2014) found that plant
78 survival in the northern Neotropical region during HS required migrations to refugia.
79 The climatically driven pace and magnitude of changes in aquatic environments can,
80 however, vary considerably relative to effects in terrestrial environments (Sandel et
81 al., 2011; Litsios et al., 2012; Bonetti and Wiens, 2014). It therefore remains
82 uncertain how aquatic species responded to past climate alterations.

83 To evaluate past biogeographic dynamics of northern Neotropical inland aquatic
84 species, we used freshwater ostracodes (bivalved microcrustaceans) as a model
85 group, and two complementary approaches (1) fossil records (Dawson et al., 2011;
86 McGuire and Davis, 2013) and (2) species distribution models (SDM) (Elith and
87 Leathwick, 2009; Nogués-Bravo et al., 2009; Veloz et al., 2012; Maguire et al., 2015).

88 Ostracodes were selected because they possess one of the best fossil records in the
89 region since the Late Quaternary (Pérez et al., 2011, 2013) and have demonstrated
90 to be sensitive to climatic variation (at modern and past). Given their intermediate
91 role on trophic chains (Valtierra-Vega and Schmitter-Soto, 2000; Bergmann and
92 Motta, 2005; Cohuo et al., 2016), changes in their abundances and assemblage
93 composition can also reflect changes in primary production and higher trophic levels.
94 Paleorecords provide true evidences for the presence of a species within the past, at
95 resolutions ranging from decadal to millennial scales, but in absence of a denser
96 spatial network, this approach is usually limited to the local scale (Maguire and
97 Stigall, 2009; Dawson et al., 2011). Species distribution models are based on the
98 combination of georeferenced species occurrences with environmental information to
99 characterize the range of climate tolerance that a species inhabits (Guisan and
100 Thuiller, 2005; Maguire et al., 2015). By using multiple time periods, species
101 occurrences across different climatic scenarios can be projected to a certain degree
102 (Elith and Leathwick, 2009; Svenning et al., 2011).

103 Most important limitations and uncertainties of SDMs are the according forcing data
104 such as GCMs and the statistical algorithms employed. For instance, simulations of



105 tropical Atlantic climates remain deficient in many climate models due to incomplete
106 characterization of the vertical structure of tropospheric water vapor and humidity. As
107 a consequence, the simulation of temperature and precipitation gradients is afflicted
108 with a high degree of uncertainty in GCM's, especially across regions with irregular
109 and complex topography (Solomon et al., 2010). Statistical algorithms and data
110 parametrization also add another level of uncertainty in the downscaling cascade,
111 including the structure of past surface fields such as topography, vegetation structure
112 and coastline. Moreover, the usage of statistical algorithms for the geospatial
113 mapping also includes uncertainties that are implicitly included in the results (Chen et
114 al., 2010; Neelin et al., 2010).

115 The combination of paleorecords and SDM's, provides a unique opportunity to obtain
116 quantitatively and potentially high-resolution reconstructions of past species
117 dynamics at local and regional scale during past climate fluctuations in the northern
118 Neotropical region.

119 In this study, we addressed three overarching questions: 1) Did past climate changes
120 since 155 ka BP (Hodell et al., 2008; Correa-Metrio et al., 2012a, b, 2014; Cohuo et
121 al., 2018) have profound consequences for aquatic ecosystem stability in the
122 northern Neotropics? 2) Did endemic and non-endemic (widespread) species
123 respond in the same way to climate shifts? 3) Did refugia exist, and if so, what was
124 their spatial distribution?

125 **2 Methods**

126 **2.1 Study area and sampling of modern species**

127 Our study area is the northernmost northern Neotropics, an area that extends from
128 southern Mexico to Nicaragua (Fig.1). We sampled 205 aquatic ecosystems during
129 2010–2013, including *cenotes* (sinkholes), lakes, lagoons, crater lakes, maars,
130 permanent and ephemeral ponds, wetlands, and flooded caves. Sampled systems
131 are located at elevations from ~10 to ~4000 m a.s.l., and conductivity ranged from
132 0.1 to 3500 $\mu\text{S cm}^{-1}$. Most aquatic systems were shallow with a mean depth < 10m,
133 except for large lakes such as Petén Itzá, Atitlán, Coatepeque, Ilopango, Lachuá,
134 crater and maar lakes and cenotes which are mostly >15m deep. Biological samples
135 were collected at three different sections of the systems; littoral, water column and
136 deepest bottom. At littoral areas, we sampled in between submerged vegetation



137 using a hand net of 250 µm open mesh. Water column was sampled doing vertical
138 tows and horizontal trawls with a net of 20 cm-wide mouth and 150 µm mesh size.
139 Sediment samples were taken from the deepest part of the systems with an Ekman
140 grab, but only the uppermost centimeters of each grab were used for further analysis.
141 Ostracodes were sorted in the laboratory using a Leica Z4 stereomicroscope and
142 dissections were carried out in 3% glycerine. Shells were mounted on
143 micropaleontological slides. Dissected appendages were mounted in Hydromatrix®
144 mounting media. Taxonomic identification followed Karanovic, (2012) and Cohuo et
145 al. (2016). Four ostracode species were selected for this study: *Cypria petenensis*
146 Ferguson et al., 1964, *Paracythereis opesta* (Brehm, 1939), representing taxa
147 endemic to the northern Neotropical region (Cohuo et al., 2016) (Fig. 1A, B), and
148 *Cytheridella ilosvayi* Daday, 1905 and *Darwinula stevensoni* (Brady & Robertson,
149 1870), which are widely distributed (non-endemic) on the American continent (Fig.
150 1C, D).

151 **2.2 Sediment cores from Lake Petén Itzá and regional paleo-records**

152

153 Information about fossil occurrences of the target species was obtained from
154 sediment cores retrieved from Lake Petén Itzá (northern Guatemala), by the Petén
155 Itzá Scientific Drilling Project (PISDP). Cores PI-1, PI-2, PI-6 (Mueller et al., 2010)
156 and Petén-Itzá 22-VIII-99 were used. Core chronologies and sampling methods can
157 be found in Kutterolf et al. (2016) and Mueller et al. (2010), respectively. Sample
158 resolution (20 cm) in each core represents ~5 ka (Mueller et al., 2010). Ostracode
159 separation methods and counting can be found Cohuo et al. (2018). We looked at
160 near-continuous ostracode fossil occurrences in the sediments over the last 155 ka.
161 There was, however, a gap in sediments availability during the period 83-53 ka BP.
162 We also compiled fossil data for our target species from 19 other studies in the
163 northern Neotropical region, to obtain past spatial distributions of the target species
164 (Supplementary material, Table S1). These studies were restricted to the LGM and
165 middle Holocene.

166 Shells of the target species were measured and photographed using a Canon
167 Powershot A640 digital camera attached to a Zeiss Axiostar-plus light microscope.



168 Abundances of the target species in each core were plotted using C2 software
169 version 1.5 (Juggins, 2007).

170 **2.3 Species niche modelling (SNM): modern projections and reconstruction of** 171 **past distributions**

172 We determined modern macro- and micro-ecological preferences for our target
173 species using our data set (multivariate approach) and the literature (Pérez et al.,
174 2010). Given the ecological preferences of the species, we used seven environmental
175 variables related to temperature and precipitation, as they have been shown to have
176 the strongest relationships with ostracode distribution: 1) mean annual temperature, 2)
177 mean diurnal temperature range, 3) isothermality (day-to-night temperature oscillation
178 relative to summer-to-winter), 4) temperature seasonality, 5) annual temperature
179 range, 6) total annual precipitation, and 7) precipitation seasonality, all available from
180 the WorldClim database (Hijmans et al., 2005; <http://www.worldclim.org>). Variables of
181 importance were analyzed to identify those with greatest influence on each ostracode
182 species distribution.

183 Environmental conditions of the present corresponded to the interpolation of average
184 monthly climate data from weather stations of various locations of the world and major
185 climate databases such as the Global Historical Climatology Network (GHCN) and the
186 Food and Agricultural Organization of the United Nations (FAO). Grids had a spatial
187 resolution of 30-arc second. Although modern climatic data is generated at very high
188 resolution, one should note that modelling of tropical climate and circulation is still
189 afflicted by a comparatively high degree of uncertainty, especially the realistic
190 simulation of the hydrological cycle and precipitation. In this context, the purpose of
191 the study is also to investigate how far differences in profound background climatic
192 changes during Glacial-Interglacial periods are responsible for lateral and/or vertical
193 changes in ecological niches of the respective species.

194 Past species distributions were investigated using climate conditions inferred for
195 three time periods: ~120 ka BP (last interglacial), ~22 ka BP (Last Glacial Maximum
196 [LGM]) and ~6 ka BP (middle Holocene). For environmental data corresponding to
197 ~120 ka BP (Otto-Bliesner et al., 2006), grids have a spatial resolution of 30-arc
198 seconds, which represents ~1 km² in the northern Neotropical region. Environmental
199 conditions at ~22 and ~6 ka BP were obtained from downscaled paleoclimatic



200 simulations forced with the coarsely resolved output fields of two global circulation
201 models (GCMs), the MIROC-ESM 2010 (Watanabe et al., 2011) and CCSM4 (Gent
202 et al., 2011).

203 These GCMs were selected because they yield slightly varying temperature and
204 differences in precipitation fields (Fig. 2). At ~22 ka BP, the MIROC-ESM model
205 shows colder and drier conditions in the region than does the CCSM4 model (Fig. 2).
206 At ~6 ka BP, the CCSM4 model simulates slightly cooler and drier conditions than
207 does the MIROC-ESM model (Fig. 2). These differences enable assessment of model
208 uncertainty with respect to global climate simulations.

209 The target grids at the lower end of the downscaling cascade have a spatial resolution
210 of 2.5-arc minutes, which represents ~5 km² in the study area. For all periods, grids
211 with global information were trimmed to match the extent of our study area. The SDM
212 toolbox (Brown, 2014), implemented in Arc GIS, was used for this purpose.

213 The modeling framework was constructed using five presence/absence-based
214 algorithms because of true species absences in our database. We used the
215 Generalized Linear Model (GLM) (McCullagh and Nelder, 1989), the Generalized
216 Additive Model (GAM) (Hastie and Tibshirani, 1990), the Generalized Boosting Model
217 (GBM) (Ridgeway, 1999), Maximum Entropy (MAXENT) (Tsuruoka, 2006) and the
218 Surface Range Envelope (SRE) (Busby, 1991). The first three algorithms, GLM, GAM
219 and GBM are regression-based models, which are flexible to handle a variety of data
220 responses types (linear and non-linear) and are less susceptible to overfitting than
221 other algorithms such as multivariate adaptive regression splines (MARS) (Guisan et
222 al., 2002; Franklin, 2010). MAXENT is a general-purpose machine learning method
223 which predicts a species probability occurrence by finding the distribution closest to
224 uniformity (maximum entropy), it requires previous knowledge of the environmental
225 conditions at known occurrence localities (Elith et al., 2011). The SRE algorithm is an
226 envelope-type method that uses the environmental conditions of locations of
227 occurrence data to profile the environments where a species can be found (Araujo
228 and Peterson 2012). All these modelling techniques are at different degree limited by
229 several numerical factors, such as missing values, outliers, sampling size, overfitting
230 and interaction between predictors. Special attention therefore must be paid to
231 produce reliable models which maximizes the agreement of the predicted species
232 occurrences with the observed data (Guisan et al., 2002; Franklin, 2010). In most



233 cases the combination of methods (e.g. GLM and GAM) is recommended to assess
234 the robustness of according results of individual models (Guisan et al., 2002).

235 For our study, settings for all modeled techniques, such as the number of trees,
236 number of permutations, iteration depths, Bernoulli distribution normalization and
237 node-size, follow George and Thuiller (2013). Records were split randomly into a
238 training (calibration) (70%) and a test (validation) (30%) dataset, with 10 replications
239 for each model type. A total of 50 models (5 algorithms and 10 replications) were
240 generated for each ostracode species and time period. All projections were evaluated
241 using three statistical approaches, to reduce uncertainty in species niche models: 1)
242 The true skill statistics (TSS), (2) the area under the receiver operating characteristic
243 curve (AUC) and (3) Cohen's Kappa statistics (Thuiller et al., 2009, 2015). For all
244 algorithms, best-fit model runs above critical values (TSS values >0.4, AUC >0.7 and
245 KAPPA >0.4) were used to construct consensus maps for each modeling technique.
246 Final maps were constructed using an ensemble of all techniques. The combination
247 of methods reduces the effect of inter-model variability and uncertainties that arise
248 from using single algorithms (Araújo and New, 2007; Marmion et al., 2009; Thuiller et
249 al., 2009). The final distribution maps thus indicate areas simulated by most modeling
250 techniques. All calculations were done using the 'biomod2' v.3.1-64 package (Thuiller
251 et al., 2015), implemented in R v.3.2.1 software (R Development Core Team, 2015).

252 **3 Results**

254 **3.1 Northern Neotropical paleorecords, species permanence and displacement**

256 Records of the period corresponding to the Last Interglacial (130-115 ka BP), were
257 obtained from core PI-7 (155-83 ka BP). Abundances of our four target species were
258 generally low, with <60 adult shells gr⁻¹, and frequencies (relative abundances) varied
259 considerably (Fig. 3). The endemic *C. petenensis* was the most frequent species (Fig.
260 3). *Paracythereis opesta* and *C. ilosvayi*, which are bottom-dwelling organisms, were
261 recovered only from sediments deposited ca. 87-85 ka BP, where high abundances of
262 *C. petenensis* were observed (Fig. 3). *Darwinula stevensoni* showed a sole
263 occurrence at ~155-153 ka BP.



264 Records of the Last Glacial and Deglacial were obtained from Lake Petén Itzá core PI-
265 2 (Fig. 4A) and published data from core PI-6 (Fig. 4B) (Pérez et al., 2011). Pérez et
266 al. (2011) found nearly continuous presence of endemic species in core PI-6 during
267 the interval 24–10 ka BP. Gaps of millennial duration are, however, evident for the
268 periods 24–22 and 13–10.5 ka BP. The record from PI-2 shows a complementary
269 pattern to that of PI-6, because species presence in PI-2 coincided with species
270 absence in core PI-6. *Cypria petenensis* in the PI-2 record, for example, shows high
271 abundances at the onset of the LGM (23–21 ka BP), and *P. opesta* displays high
272 abundances around 22 and 19 ka BP (Fig. 4A). Thus, the two records suggest
273 continuous presence of endemic species in Lake Petén Itzá during both the LGM and
274 Deglacial.

275 Non-endemic species show intermittent distributions in both the PI-2 and PI-6 cores
276 (Fig. 4A, B). *Darwinula stevensoni* was recorded exclusively at ca. 23, 22–20, and 19–
277 18 ka BP, the latter at the onset of the Deglacial. Similarly, *Cytheridella ilosvayi* was
278 present in very low abundances during two short episodes at about 20 and 14 ka BP.
279 We recorded low abundances of both species during the LGM (<250 adult shells g⁻¹),
280 compared to periods immediately before and after, when temperatures are thought to
281 have been warmer. For example, during the Deglacial, abundances were always >250
282 adult shells g⁻¹.

283 Fossil records from the middle Holocene were obtained from core Petén-Itzá 22-VIII-
284 99 and eleven regional studies (Fig. 5A). The record from core Petén-Itzá 22-VIII-99,
285 retrieved from 11.5 m water depth, shows that endemic species were present
286 continuously during the last 6.5 ka (Fig. 5A). Most regional records came from
287 cenotes and lakes on the Yucatán Peninsula (Supplementary material, Table S1). All
288 fossil records show that endemic species were spatially distributed throughout the
289 current ranges of extant populations (Fig. 5B).

290 For non-endemic species, regional fossil records from the middle Holocene revealed
291 their presence ranging from the northern Yucatán Peninsula to northern Guatemala
292 and Belize (Supplementary material, Table S1). Core Petén-Itzá 22-VIII-99 highlights
293 an almost continuous presence of *C. ilosvayi* in the lake, characterized by high
294 abundances, except for the period 11–8.5 ka BP, when the species was absent (Fig.
295 5A). *Darwinula stevensoni* was present continuously during the last 9 ka, but in the
296 lower section of the core, dated to 14–10 ka BP, the species was absent (Fig. 5A).



297 **3.2 Species niche modeling: distribution hindcasting for time slices ~120, ~22**
298 **and ~6 ka BP**

299

300 For the 205 aquatic ecosystems sampled, 145 had at least one of the target species
301 present: *C. petenensis*, *P. opesta*, *C. ilosvayi* and *D. stevensoni*. Forty-nine systems
302 contained *C. petenensis*, 37 had *P. opesta*, 79 were inhabited by *C. ilosvayi*, and 61
303 contained *D. stevensoni*. Analysis of variables of importance showed that
304 environmental variables with the greatest influence on species distribution are
305 precipitation seasonality and mean annual temperature (Table 1). For individual
306 species, however, variables received different scores, indicating that each species
307 optimal climate niche is controlled by a particular combination of variables (Table 1).
308 Diagnostic tests of the reconstructions (TSS, AUC and Kappa) show good
309 performance for all algorithms and periods evaluated (Table 1). There were,
310 however, differences in predictive accuracy within species. Modeled distributions of
311 endemic species have the highest evaluation scores (AUC =0.8, TSS=0.49,
312 Kappa=0.45). Non-endemic species models (AUC=0.75, TSS=0.46, Kappa=0.46)
313 have slightly lower values, but also fall within the acceptable range.

314 Reconstructions for the period ~120 ka BP suggest very broad distributions of
315 endemic taxa, as climate enabled the species to expand their ranges. Probability
316 values, however, were relatively low (<80%) (Fig. 3B). For the non-endemic species,
317 reconstructions for ~120 ka BP show different areas of climatic suitability, with species
318 presence probabilities reaching 60%. Zones of higher probability (>80%) are
319 dispersed throughout the region. The most extensive zones of species distribution
320 suitability are located along the Caribbean coast of the Yucatán Peninsula and in
321 northern Guatemala (Fig. 3B).

322 Inferences for endemic taxa distributions at ~22 ka BP, based on the CCSM4 model,
323 suggest that these species remained in the core area, but that they may have been
324 displaced somewhat to the northern portion of the Yucatán Peninsula (Fig. 4C). This
325 estimate has probability values of >75%. The MIROC-ESM model suggests areas of
326 distribution similar to those presented by the CCSM4 model, but slightly more
327 restricted areas for *C. petenensis* and more widespread areas for *P. opesta*.
328 Probability values were low in this model (<65%) (Supplementary material, Fig. S1).
329 Models for non-endemic species reveal fragmented and discontinuous distributions
330 (Fig. 4C). At ~22 ka BP, corresponding to the LGM, both the CCSM4 and MIROC-



331 ESM models suggest that non-endemics moved northward on the Yucatán Peninsula
332 to the Gulf of Mexico (>65% probability), and/or were displaced southward to Central
333 America (85% probability) (Fig. 4C; Supplementary material, Fig. S1).

334 For ~6 ka BP, the CCSM4 model suggests discontinuous areas of distribution on the
335 Yucatán Peninsula (Fig. 5B) for endemic species, whereas the MIROC-ESM shows
336 more continuous distributions, particularly along the eastern portion of the Peninsula
337 (Supplementary material, Fig. S1). For non-endemic species, the CCSM4 and
338 MIROC-ESM models show very similar patterns. Extensive regions of climatic
339 suitability were identified for *C. ilosvayi*, but those with higher probability are located
340 along the Caribbean Coast (Fig. 5B; Supplementary material, Fig S1). For *D.*
341 *stevensoni*, areas of maximum probability are discontinuous. Maximum probability
342 was found at isolated regions such as the southern part of the northern Yucatán
343 Peninsula, Belize and eastern Honduras (Fig. 5B).

344

345 **4 Discussion**

346

347 **4.1 Congruence between paleo-records and modeled paleo-distributions of** 348 **freshwater ostracodes in the northern Neotropical region**

349 Our study highlights the fact that accuracy and congruence between paleo-records
350 and modeled paleo-distributions of freshwater ostracodes in the northern Neotropical
351 region was influenced by multiple factors such as climate model used, modeling
352 algorithm employed, sediment core characteristics and target species.

353 For instance, distribution models and modelling cascade were characterized by high
354 degree of uncertainty with regard of precipitation and temperature estimations of
355 climate models (GCMs). This limited the full estimation of spatial distribution of target
356 species, especially during older periods such as LIG and LGM were fossil evidence
357 (spatial and temporal) was scarce.

358 The simulation of precipitation of GCMs is afflicted with high degrees of uncertainties,
359 because the vertical structure of stratospheric water vapor and humidity profile have
360 large biases, especially in the tropics (Gettelman et al., 2010). This implies that GCMs
361 commonly reproduce large-scale pattern of precipitation with high confidence but
362 models tend to underestimate the magnitude of precipitation change at regional or



363 local scale (Stephens et al., 2010). Similarly, GCMs temperature estimations in the
364 tropics may display large biases, because changes in climate drivers of continental
365 temperature of the northern Neotropics such as Atlantic sea surface temperature and
366 the Atlantic warm pool, are usually underestimated (Liu et al., 2013). Simulations of
367 temperature variations during LGM, for example, tend to overestimate cooling in
368 tropical regions (Kageyama et al., 2006; Otto-Bliesner et al., 2009).

369 In our study, reconstructed maps based on MIROC-ESM and CCSM4 models,
370 simulate slightly different areas of distribution for the target species. This is associated
371 to differences in precipitation and temperature estimations between models. The most
372 important difference between their respective reconstructions pertains to the extent of
373 suitable areas of distribution of the species, being generally broader in MIROC-ESM
374 model than in CCSM4 model.

375 The scarcity of fossil records also limited the full reconstruction of distribution
376 dynamics of species, especially during LIG and LGM, because records were obtained
377 only from Lake Petén Itzá and were relatively scarce. The period 24-14 ka BP, was
378 highly informative, because the comparisons between cores PI-2 and PI-6, and
379 specifically, the compensation effect between them (the presence of species in a core
380 in periods where absences were determined in the other), highlight that gaps in the
381 fossil record may be related to core location in the lake, shell preservation and
382 individual species ecology and not only by species absence. This therefore, suggest
383 that short gaps, lasting less than 10 ka cannot be considered evidence for species
384 absence.

385 In general, the comparison between species distribution models and paleorecords
386 shows a quite high degree of similarity. This is especially evident for the middle
387 Holocene as the individual SMD output of the target species were compared with the
388 fossil records at regional scale. In all cases, SDMs reconstructions shows
389 distributional areas where fossil records were recovered. This congruence may be
390 supported by the agreement between estimations of temperature in climate models
391 and paleorecords.

392



393 **4.2 Endemic and non-endemic species responses during long-term climatic**
394 **fluctuations: Glacial/Interglacial cycles and Marine Isotope Stages**

395 Paleoclimate inferences derived from Lake Petén Itzá sediments suggest that
396 Glacial/Interglacial cycles in the northern Neotropical region did not have profound
397 consequences with respect to the spatial distribution of isotherms in terrestrial
398 environments (Hodell et al., 2008; Pérez et al., 2011; Escobar et al., 2012; Pérez et
399 al., 2013). Most paleoclimate studies in the region based in different proxies such as
400 ostracods, pollen, and $\delta^{18}\text{O}$ fluid inclusion data from speleothems suggest that
401 temperatures during the last glacial and start of the deglacial may have been up to
402 5°C lower than today (Correa-Metrio et al., 2012a, b; Arienzo et al., 2015; Cohuo et
403 al., 2018), although some estimations suggest a temperature depression of about
404 10°C compared with modern records (Hodell et al., 2012; Grauel et al., 2016).
405 Precipitation was affected more profoundly, but not consistently during glacial-
406 interglacial cycles and likely fluctuated in response to changes in local atmospheric
407 circulation. For instance, the position of the Hadley cell and ITCZ, together with
408 climate forcing, such as Heinrich Stadials, seem to drive precipitation fluctuation
409 locally. During the LGM, for example, humid conditions has been estimated to the
410 region (Cohuo et al., 2018).

411 Our results, however, suggest that temperature fluctuations affected aquatic species
412 associations to a higher degree compared to reductions in precipitation (changes in
413 lake water chemistry), because presence/absence of species and fluctuations in total
414 abundances match periods of temperature change, rather than times of lake level
415 shifts.

416 Endemic and non-endemic species responded similarly to Glacial and Interglacial
417 cycles and transitions. Fossil records from Lake Petén Itzá sediment cores PI-1, PI-2,
418 PI-6, and Petén-Itzá 22-VIII-99 reveal that endemic species were almost continuously
419 present during the last 155 ka. Short gaps, lasting less than 10ka were not considered
420 evidence for species absence.

421 Non-endemic species show patterns of expansion and contraction that track
422 temperature fluctuations. Modeled paleo-distributions and paleo-records show that
423 distributions of non-endemic species were widespread during the LIG and
424 fragmented during the middle Holocene, when climates were warmer. During the Last
425 Glacial, non-endemic species were absent or sporadically present. This may result in



426 response to lower temperatures characterized the LG. Modeled paleo-distributions
427 for the LGM also show that non-endemic species were displaced from their current
428 ranges toward the northern Yucatán Peninsula and/or southward toward Central
429 America, where a warm climate likely persisted. This scenario suggests migrations of
430 regional magnitude, as species were lost from areas such as southern Mexico and
431 northern Guatemala but persisted within their current range of distribution in
432 fragmented populations, such as areas of southeast Honduras and northeast
433 Nicaragua.

434 The presence of endemics and absence of non-endemic species during the LGM,
435 reveal a clear ecological signal, which may be associated to the degree of adaptation
436 to ecological niches. Endemic species seem to be highly resilient to long-term natural
437 disturbances, whereas non-endemic demonstrated to be more sensitive. There is
438 increasing evidence that biological communities, particularly terrestrial taxa, display
439 strong resilience in the face of natural and human disturbances in the northern
440 Neotropical region. Hurricane impacts, widespread pre-Columbian agricultural
441 activities, and decadal-to-centennial climate changes are recognized as main
442 disrupters of Holocene ecosystem composition and function in the region. Such
443 perturbations, however, did not severely and permanently alter plant associations
444 such as moist forests (Bush and Colinvaux, 1994; Cole et al., 2014) and dry tropical
445 forests (Van Bloem et al., 2006; Holm 2017), which persisted in the region despite
446 these disturbances. Plant taxa of Panama demonstrated a recovery time of just
447 350yrs after strong deforestation by pre-Columbian agriculture (Bush and Colinvaux,
448 1994). Similarly, the rain forest in Guatemala recovered from Mayan alterations in a
449 time span of 80-260yrs (Mueller et al., 2010). Bird composition have also
450 demonstrated rapid recovery time after hurricane impacts, species compositions
451 affected in Central America and the Caribbean return to pre-hurricane conditions in
452 time periods ranging from months to years (Will, 1991, Wunderle et al., 1992;
453 Johnson and Winker, 2010).

454

455 The continuous presence of both endemic and non-endemic (except during the LGM)
456 ostracode species in the northern Neotropics during Glacial/Interglacial cycles, also
457 reflects the fact that aquatic ecosystem functionality was little altered during the last
458 155 ka. High abundance of ostracodes, which belong to intermediate trophic levels,



459 suggests high rates of primary production and ample food sources for higher
460 consumers, especially during the LIG and middle Holocene. During the LGM, the
461 presence of endemics and absence of non-endemics, along with lower total
462 ostracode abundances, suggest moderate alteration of aquatic ecosystem dynamics.
463 Reduced primary production and loss of poorly adapted species might also be
464 inferred for this period.

465 Marine Isotope Stages (MISs), which describe shorter periods of (marine) climate
466 variability (cooling and warming) than terrestrial Glacial/Interglacial cycles, were also
467 used to evaluate the distribution dynamics of aquatic species. During MISs, ostracode
468 composition remained relatively constant, even across MIS boundaries (Fig. 6).
469 Sediments from Lake Petén Itzá that correspond to warmer periods MIS3 (57-29 ka
470 BP) and MIS1 (14 ka BP to present) were characterized by abundant fossils. MIS2
471 (29-14 ka BP) shows lower species abundances (total adult and juvenile valves), likely
472 related to persistent cold temperatures. The absence of *Cytheridella ilosvayi* during
473 most of MIS2 illustrates the sensitivity of non-endemics to cool temperatures (Fig. 6).
474 Similar to Glacial/Interglacials in terrestrial environments, during MISs, northern
475 Neotropical endemic species showed high resilience to changes between cold and
476 warm phases, whereas non-endemic species proved to be more sensitive to cold
477 periods, especially the LGM.

478 **4.3 Species responses during abrupt climate shifts, and refugia for aquatic taxa**

479 Fossil records from Lake Petén Itzá suggest that the periods of strongest climatic
480 fluctuations during the last 155 ka BP in the northern Neotropics occurred around 85
481 ka BP (Mueller et al., 2010) and Heinrich Stadials (Correa-Metrio et al., 2012b; Cohuo
482 et al., 2018). Those episodes were characterized by dramatic decreases in lake level,
483 suggesting intense aridity in the region. Lowest estimated temperatures (5-10 °C
484 lower than today) for the entire record correspond to HS1.

485 Correa-Metrio et al. (2013) estimated high climate change velocity in the region during
486 HS1, which produced large changes in terrestrial plant communities. Correa-Metrio et
487 al. (2012b, 2014) estimated that one of the consequences of such ecological
488 instability was the substantial migration of tropical vegetation and development of
489 refugia. The high velocity of climate change inferred for the northern Neotropical
490 region is, however, opposite to trends observed elsewhere in the tropics, which
491 suggest that high biodiversity and endemism are associated with low climate change



492 velocities and high species resilience (Sandel et al., 2011). It remains uncertain how
493 climate change velocity during period of abrupt climate change affected aquatic
494 communities in the northern Neotropical region. It is also unclear whether aquatic taxa
495 were as dramatically affected as local terrestrial species during these abrupt episodes,
496 or if they simply displayed high resilience.

497 We analyzed the HS1 structure in detail, because that was the period of coldest
498 temperatures and extreme drought during the last 85 ka (Mueller et al., 2010; Correa-
499 Metrio et al., 2012a; Cohuo et al., 2018). Mueller et al. (2010) estimated that Lake
500 Petén Itzá water level decreased by ~50 m during that period, which would imply that
501 lakes in the region with maximum depths <50 m, dried completely.

502 Modeled paleo-distributions suggest that with respect to temperature fluctuations
503 during HS1, conditions remained suitable for tropical species (especially endemics)
504 across large areas of the Yucatán Peninsula and in northern Central America. We
505 assume that lakes that held water during HS1 served as “refugia” for aquatic taxa, as
506 temperature apparently did not limit species distributions (Cohuo et al., 2018).

507 Systems such as *cenotes* and lakes that are not directly dependent on precipitation to
508 maintain water level, but are instead controlled by large subterranean aquifers (Perry
509 et al., 2002; Schmitter-Soto et al., 2002; Vázquez-Domínguez and Arita, 2010) may
510 serve as “refugia” for aquatic species, enabling native species to remain in the region
511 during periods of low rainfall. To date, it remains uncertain whether lakes and *cenotes*
512 (approximately 7,000 in the Yucatán Peninsula) held water during HS1, and little is
513 known about their spatial distribution. Isolated water bodies (refugia) may explain the
514 high percentage of endemism and micro-endemism (species distributed in a single or
515 limited group of lakes) for aquatic taxa on the northern Yucatán Peninsula (Mercado-
516 Salas et al., 2013). Species that inhabited such systems may have remained isolated
517 and adapted to specialized environmental niches.

518 Deevey et al. (1983) studied sediment cores from Lakes Salpetén ($Z_{\max} = \sim 30$ m) and
519 Quexil ($Z_{\max} = \sim 30$ m), Guatemala, and inferred that most lakes, including *cenotes*, in
520 the northern Neotropics dried out during the Deglacial because of the hydrological
521 sensitivity of the region. They also found that most lake sediment cores from the
522 region bottom out at ~8 ka BP, which means that the lakes probably first filled in the
523 early Holocene, in response to wetter conditions and rising sea level, which raised the



524 local water table. The authors therefore suggested that only large lakes in the region,
525 with maximum depths >50 m (e.g. Petén Itzá, Macaniché, Atitlán, Coatepeque,
526 Ilopango) held water during the dry Deglacial, but possessed water chemistry much
527 different from today, which limited habitats for aquatic species.

528 This second scenario favors the hypothesis of central populations (meta-populations)
529 in one or more large lakes, which enabled species exchange with surrounding aquatic
530 environments, thereby preventing species losses in small populations by demographic
531 stochasticity. The two scenarios are not mutually exclusive, and it is possible that both
532 account for the success of aquatic tropical taxa through periods of abrupt or prolonged
533 climate fluctuations. Lake Petén Itzá may have played an important role for aquatic
534 species survival and dispersal in the northern Neotropical region, because it held
535 water for at least the last 400 ka (Kutterolf et al., 2016).

536 Our findings contrast with results from terrestrial environments, which show that HS1
537 drove plant species to migrate and retreat to a few well-defined micro-refugia (Cavers
538 et al., 2003; Dick et al., 2003; Correa-Metrio et al., 2013). Burrows et al. (2011)
539 demonstrated that the pace of climate shifts in aquatic and terrestrial systems can be
540 very different. They estimated that vegetation responds rapidly to climate change,
541 especially to precipitation and temperature shifts. Indeed, changes in these variables
542 can alter the composition of vegetation abruptly, within a few years. Conversely, in
543 aquatic environments, the velocity of climate change tends to be slower. For instance,
544 given the geomorphology of water systems in the region such as cenotes (small area
545 <1km², and deep waters >10m) and large lakes as Petén Itzá (>120m deep), dramatic
546 changes in air temperatures are needed to alter the temperature of the water column
547 and thus impact species niche stability. Our study suggests that the velocity of change
548 in aquatic environments remained low in the northern Neotropical region, enabling
549 local species to adapt and specialize to their environments instead of migrating and/or
550 remaining isolated in refugia, as observed in tropical areas elsewhere.

551 **5 Conclusion**

552 Our study integrates species distribution models and paleorecords to reconstruct
553 aquatic species distribution dynamics during the last 155ka BP in the northern
554 Neotropics. Both approaches show strengths and limitations. Species distribution
555 models were afflicted by a degree of uncertainty due to uncertainties of general



556 circulation models MIROC-ESM and CCSM4 simulations related to precipitation and
557 temperature. Although these uncertainties can be considered as systematic errors, it
558 remains uncertain whether the lower-end simulations based on SDMs generated in
559 this study, fully reconstruct suitable areas of distribution of aquatic species, especially
560 because in tropical regions the larger biases on simulated values of precipitation and
561 temperature have been estimated.

562 Most important limitations of paleorecords relate to the scarcity of fossil evidence
563 spatially and temporally, especially for the older periods evaluated. Low abundances
564 in ostracodes were associated to species ecological preferences, core location and
565 preservation processes. The integration of fossil evidence from two long cores of the
566 Lake Petén Itzá was highly informative as the full range of temporal
567 presence/absence of the target species were recovered.

568 In spite, limitations of both approaches, the comparison of SDM outputs and fossil
569 records, resulted in congruent patterns. For the older periods such as LIG and LGM
570 temporal agreement between approaches was observed. For the most recent period
571 (middle Holocene) temporal and spatial agreement were observed.

572 Given the congruence between approaches, our study highlights the following
573 conclusions:

574 1.- Distribution dynamics of endemic and non-endemic species result in similar
575 patterns throughout long-term climatic fluctuations such as Glacial/Interglacial cycles
576 and Marine Isotope Stages.

577 2.- More divergent patterns can be observed during episodes of profound climatic
578 alterations such as LGM and HS1.

579 3.- Endemic species are highly resilient and remained in the core area during periods
580 of strong alteration of temperature and precipitation.

581 4.- Non-endemic species are sensitive to decreases of temperature, being displaced
582 to Central America to track climates compatible with their tolerance ranges.

583 This study represents to our knowledge the first insight into the magnitude of
584 ecological alteration of aquatic ecosystems during different past climatic scenarios in
585 the northern Neotropical region. Further studies may therefore consider refining the



586 spatial and temporal resolutions of the analyses and incorporate additional lines of
587 evidence such as molecular data. The understanding of historical species dynamics
588 can help to generate strategies for the protection of the biota which can be highly
589 threatened by the future emergence of non-analogous climates.

590 **Acknowledgment**

591
592 We thank all our colleagues who were involved in this work, including: 1) the student
593 team from the Instituto Tecnológico de Chetumal (Mexico) (Christian Vera, León E.
594 Ibarra, Miguel A. Valadéz, Cuauhtémoc Ruiz), 2) Ramón Beltrán (Centro
595 Interdisciplinario de Ciencias Marinas, Mexico), and 3) Lisa Heise (Universidad
596 Autónoma de San Luis Potosí, Mexico), for their excellent work in the field. We also
597 thank the following colleagues who provided support for sampling: 1) Manuel Elías
598 (El Colegio de la Frontera Sur, Chetumal Unit, Mexico), 2) Alexis Oliva and the team
599 from the Asociación de Municipios del Lago de Yojoa y su área de influencia
600 (AMUPROLAGO, Honduras), 3) María Reneé Álvarez, Margarita Palmieri, Leonor de
601 Tott, Roberto Moreno (Universidad del Valle de Guatemala, Guatemala), 4)
602 Personnel of the Consejo Nacional de Áreas Protegidas (CONAP, Guatemala), 5)
603 Néstor Herrera and colleagues from the Ministerio de Medio Ambiente (San
604 Salvador, El Salvador). Funding was provided by the Deutsche
605 Forschungsgemeinschaft (DFG, SCHW 671/16-1) and Technische Universität
606 Braunschweig. CONACYT (Mexico) provided fellowships (218604, 218639) to the
607 first two authors.

608

609 Author contributions.

610 SC, LMG and KN designed species distribution models and carried them out. LGM
611 and SW provided data for model parametrization and validation. LP, PE, MB, JC
612 provide data on fossil assemblages for the periods LGM and middle Holocene. SC,
613 LMG and AS prepared the manuscript with contributions from all co-authors.

614 Competing interests.

615 The authors declare that they have no conflict of interest.

616

617



618 **References**

619

620 Araújo, M., and New, M.: Ensemble forecasting of species distributions, *Trends Ecol. Evol.*,
621 22, 42–47, <https://doi.org/10.1016/j.tree.2006.09.010>, 2007.

622

623 Bonetti, M.F., and Wiens, J.J.: Evolution of climatic niche specialization: a phylogenetic
624 analysis in amphibians, *Proc Biol Sci.*, 281, (1795), <https://doi.org/10.1098/rspb.2013.3229>,
625 2014.

626

627 Brown, J.L.: SDMtoolbox: a python-based GIS toolkit for landscape genetic, biogeographic,
628 and species distribution model analyses, *Methods Ecol. Vol.*, 5, 694–
629 700. <https://doi.org/10.1111/2041-210X.12200>, 2014.

630

631 Burrows, M.T., Schoeman, D.S., Buckley, L.B., Moore, P., Poloczanska, E.S., Brander, K.M.,
632 Brown, C. Bruno, J.F., Duarte, C.M., Halpern, B.S., Holding, J., Kappel, C.V., Kiessling, W.,
633 O'Connor, M.I., Pandolfi, J.M., Parmesan, C., Schwing, F.B., Sydema W.J., and
634 Richardson, A.J.: The pace of shifting climate in marine and terrestrial
635 ecosystems, *Science*, 334, 652–655, <http://doi.org/10.1126/science.1210288>, 2011.

636

637 Busby, J.R.: BIOCLIM – a bioclimate analysis and prediction system, *Plant Prot. Q.*, 6, 8–
638 9, 1991.

639

640 Bush, M.B., Correa-Metrio, A.Y., Hodell, D.A., Brenner, M., Anselmetti, F.S., Ariztegui,
641 Mueller, D.A.D., Curtis, J.H., Grzesik, D.A., Burton, C., and Gilli, A.: Re-evaluation of climate
642 change in lowland Central America during the Last Glacial Maximum using new sediment
643 cores from Lake Petén Itzá, Guatemala, in *Climate Variability in South America and*
644 *Surrounding Regions from the Last Glacial Maximum to the Holocene*, edited by: Vimeux, F.,
645 Sylvestre, F., Khodri, M., Past Springer, Netherlands, 113–28, [https://doi.org/10.1007/978-](https://doi.org/10.1007/978-90-481-2672-9_5)
646 [90-481-2672-9_5](https://doi.org/10.1007/978-90-481-2672-9_5), 2009.

647

648 Bush, M. B., and Colinvaux, P.A.: A paleoecological perspective of tropical forest disturbance:
649 records of Darien Panama, *Ecology*, 75, 1761–1768,
650 <https://www.jstor.org/stable/1939635>, 1994.

651

652 Cavers, S., Navarro, C., and Lowe, A.J.: Chloroplast DNA phylogeography reveals
653 colonization history of a Neotropical tree, *Cedrela odorata* L., in Mesoamerica, *Mol. Ecol.*, 12,
654 1451–1460, <https://doi.org/10.1046/j.1365-294X.2003.01810.x>, 2003.

655



- 656 Cohuo, S., Macario-González, L., Pérez L., and Schwalb, L.: Overview of Neotropical-
657 Caribbean freshwater ostracode fauna (Crustacea, Ostracoda): identifying areas of
658 endemism and assessing biogeographical affinities, *Hydrobiologia*, 1–17,
659 <https://doi.org/10.1007/s10750-016-2747-1>, 2016.
- 660
- 661 Cohuo, S., Macario-González, L., Pérez, L., Sylvestre, F., Paillès, C., Curtis, J., Kutterolf, S.,
662 Wojewódka, M., Zawisza, E., Szeroczyńska, K., and Schwalb, A.: Ultrastructure and aquatic
663 community response to Heinrich Stadial (HS5a-HS1) in the continental northern Neotropics,
664 *Quat. Sci. Rev.*, 19, 75–91, <https://doi.org/10.1016/j.quascirev.2018.07.015>, 2018.
- 665
- 666 Cole, L.E., Bhagwat, S.A., and Willis K.J.: Recovery and resilience of tropical forests after
667 disturbance, *Nat. Commun.*, 5, 3906, <https://doi.org/10.1038/ncomms4906>, 2014.
- 668
- 669 Correa-Metrio, A., Bush, M., Lozano-García S., and Sosa-Nájera, S.: Millennial-Scale
670 Temperature Change Velocity in the Continental Northern Neotropics, *PLoS ONE* 8, 12,
671 e81958, <https://doi.org/10.1371/journal.pone.0081958>, 2013.
- 672
- 673 Correa-Metrio, A., Bush, M., Cabrera, K., Sully, S., Brenner, M., Hodell, D., Escobar J., and
674 Guilderson, T.: Rapid climate change and no-analog vegetation in lowland Central America
675 during the last 86,000 years, *Quat. Sci. Rev.*, 38, 63–75,
676 <https://doi.org/10.1016/j.quascirev.2012.01.025>, 2012a.
- 677
- 678 Correa-Metrio, A., Bush, M.B., Hodell, D.A., Brenner, M., Escobar, J., and Guilderson, T.:
679 The influence of abrupt climate change on the ice-age vegetation of the Central American
680 lowlands, *J. Biogeogr.*, 39, 497–509, <https://doi.org/10.1111/j.1365-2699.2011.02618.x>,
681 2012b.
- 682
- 683 Correa-Metrio, A., Meave, J.A., Lozano-García S., and Bush, M.B.: Environmental
684 determinism and neutrality in vegetation at millennial time scales, *J. Veg. Sci.*, 25, 627–635,
685 <https://doi.org/10.1111/jvs.12129>, 2014.
- 686
- 687 Dawson, T.P., Jackson, S.T., House, J.I., Prentice, I.C., and Mace G.M.: Beyond Predictions:
688 Biodiversity Conservation in a Changing Climate, *Science*, 332, 53–58,
689 <https://doi.org/10.1126/science.1200303>, 2011.
- 690
- 691 Deevey, E.S., Brenner, M., and Binford, M.W.: Paleolimnology of the Petén district,
692 Guatemala, *Hydrobiologia*, 103, 205, <https://doi.org/10.1007/BF00028453>, 1983.



693
694 Dick, C.W., Abdul-Salim K., and Bermingham, E.: Molecular systematic analysis reveals
695 cryptic Tertiary diversification of a widespread tropical rain forest tree, *Amer. Naturalist*, 162,
696 691–703, <https://doi.org/10.1086/379795>, 2003.
697
698 Elith, J., and Leathwick, J.: Species Distribution Models: Ecological Explanation and
699 Prediction Across Space and Time, *Annu. Rev. Ecol. Evol. Syst.*, 40, 677–97,
700 <https://doi.org/10.1146/annurev.ecolsys.110308.120159>, 2009.
701
702 Escobar, J., Hodell, D.A., Brenner, M., Curtis, J.H., Gilli, A., Mueller, A.D., Anselmetti, F.S.,
703 Ariztegui, D., Grzesik, D.A., Pérez L., Schwalb, A., and Guilderson, T.P.: A ~43ka record of
704 paleoenvironmental change in the Central American lowlands inferred from stable isotopes of
705 lacustrine ostracods, *Quat. Sci. Rev.*, 37, 92–104,
706 <https://doi.org/10.1016/j.quascirev.2012.01.020>, 2012.
707
708
709 Gent, P.R., Danabasoglu, G., Donner, L.J., Holland, M.M., Hunke, E.C., Jayne, S.R.,
710 Lawrence, D.M., Neale, R.B., Rasch, P.J., Vertenstein, M., Worley, P.H., Yang, Z.L., and
711 Zhang, M.: The Community Climate System Model Version 4, *J. Clim.*, 24, 4973–4991,
712 <https://doi.org/10.1175/2011JCLI4083.1>, 2011.
713
714 Hastie, T.J. and Tibshirani, R.J.: *Generalized additive models*, CRC Press: Boca Raton, FL,
715 1990.
716
717 Hijmans, R.J., Cameron, S., Parra, K., Jones, P., and Jarvis, A.: Very high resolution
718 interpolated climate surfaces for global land areas. *Int. J. Climatol.*, 25, 1965–1978,
719 <https://doi.org/10.1002/joc.1276>, 2005.
720
721 Hodell, D.A., Anselmetti, F., Ariztegui, D., Brenner, M., Curtis, J., Gilli, A., Grzesik, D.,
722 Guilderson, T., Müller, A., Bush, M., Correa-Metrio, A., Escobar, J., and Kutterolf, S.: An 85-
723 ka record of climate change in lowland Central America, *Quat. Sci. Rev.*, 27, 1152–1165,
724 <https://doi.org/10.1016/j.quascirev.2008.02.008>, 2008.
725
726 Hodell, D.A., Turchyn, A.J., Wiseman, C.V., Escobar, J., Curtis, J.H., Brenner, M., Gilli, A.,
727 Anselmetti, F., Ariztegui, D., Perez, L., Schwalb, A., and Brown, E.: Late glacial temperature
728 and precipitation changes in the lowland Neotropics by tandem measurements of $\delta^{18}\text{O}$ in



- 729 biogenic carbonate and gypsum hydration water, *Geochim. Cosmochim. Acta*, 77, 352–368,
730 <https://doi.org/10.1016/j.gca.2011.11.026>, 2012.
- 731
- 732 Holm, J., Van Bloem, S.J., Larocque, G.R., and Shugart, H.: Shifts in biomass and
733 productivity for a subtropical dry forest in response to simulated elevated hurricane
734 disturbances, *Environ. Res. Lett.*, 12, 025007, <https://doi.org/10.1088/1748-9326>, 2017.
- 735
- 736 Holmgren, K., Lee-Thorp, J.A., Cooper, G.R.J., Lundblad, K., Partridge, T.C., Scott, L.,
737 Sithaldeen, R., Siep Talma A. and Tyson, P.D.: Persistent millennial-scale climatic variability
738 over the past 25,000 years in southern Africa, *Quat. Sci. Rev.*, 22, 2311–2326,
739 [https://doi.org/10.1016/S0277-3791\(03\)00204-X](https://doi.org/10.1016/S0277-3791(03)00204-X), 2003.
- 740
- 741 Hugall, A., Moritz, C., Moussalli A. and Stanisc, J.: Reconciling paleodistribution models and
742 comparative phylogeography in the Wet Tropics rainforest land snail *Gnarosophia*
743 *bellendenkerensis* (Brazier 1875), *Proc. Natl. Acad. Sci. U.S.A.*, 99, 6112–6117,
744 <https://doi.org/10.1073/pnas.092538699>, 2002.
- 745
- 746 Juggins S.: C2 version 1.5 user guide. Software for ecological and palaeoecological data
747 analysis and visualization, Newcastle University, Newcastle upon Tyne, UK, 2007
- 748
- 749 Karanovic, I. (Eds.): *Recent Freshwater Ostracods of the World, Crustacea, Ostracoda,*
750 *Podocopida*, Springer, Berlin, 2012.
- 751
- 752 Kutterolf, S., Schindlbeck, C., Anselmetti, S., Ariztegui, D., Brenner, M., Curtis, J., Schmid, D.,
753 Hodell, A., Mueller, A., Pérez, L., Pérez, W., Schwalb, A., Frische, M., Wang, L.: A 400-ka
754 tephrochronological framework for Central America from Lake Petén Itzá (Guatemala)
755 sediments, *Quat. Sci. Rev.*, 150, 200–220, <https://doi.org/10.1016/j.quascirev.2016.08.023>,
756 2016.
- 757 Litsios, G., Pellissier, L., Forest, F., Lexer, C., Pearman, P.B., Zimmermann, N.E., and
758 Salamin, N.: Trophic specialization influences the rate of environmental niche evolution in
759 damselfishes (Pomacentridae), *Proc. Royal Soc. Lond.*, 279, 3662–
760 3669, <https://doi.org/10.1098/rspb.2012.1140>, 2012.
- 761
- 762 Loarie, S.R., Duffy, P.B., Hamilton, H., Asner, G.P., Field, C.B., and Ackerly, D.D.: The
763 velocity of climate change, *Nature*, 462, 1052–1055, <https://doi.org/10.1038/nature08649>,
764 2009.



765
766 Maguire, K.C., Nieto-Lugilde, D., Fitzpatrick, M.C., Williams, J.W., Blois, J.L.: Modeling
767 species and community responses to past, present, and future episodes of climatic and
768 ecological change. *Annu. Rev. Ecol. Evol. Syst.*, 46, 343–368,
769 <https://doi.org/10.1146/annurev-ecolsys-112414-054441> , 2015.
770
771 Marmion, M., Parviainen, M., Luoto, M., Heikkinen, R.K., and Thuiller, W.: Evaluation of
772 consensus methods in predictive species distribution modelling, *Divers. Distrib.*, 15, 59–69,
773 <https://doi.org/10.1111/j.1472-4642.2008.00491.x>, 2009.
774
775
776 Martínez-Meyer, E., Peterson, A., and Hargrove, W.: Ecological niches as stable
777 distributional constraints on mammal species, with implications for Pleistocene extinctions
778 and climate change projections for biodiversity, *Glob. Ecol. Biogeogr.*, 13, 305–314,
779 <https://doi.org/10.1111/j.1466-822X.2004.00107.x>, 2004.
780
781 McCullagh, P. and Nelder, J.A (Eds.): *Generalized linear models.* Chapman & Hall/CRC
782 monographs on Statistics & Applied Probability, Chapman and Hall/CRC Press, London,
783 1989.
784
785 McGuire, J.L., and Davis, E.B.: Using the palaeontological record of *Microtus* to test species
786 distribution models and reveal responses to climate change, *J. Biogeogr.*, 40, 1490–500,
787 <https://doi.org/10.1111/jbi.12106>, 2013.
788
789 Mercado-Salas, NF., Morales-Vela, B., Suárez-Morales, E., and Iliffe, TM.: Conservation
790 status of the inland aquatic crustaceans in the Yucatan Peninsula, Mexico: shortcomings of a
791 protection strategy, *Aquat. Conserv.: Mar. Freshw. Ecosyst.*, 23, 939–951,
792 <https://doi.org/10.1002/aqc.2350>, 2013.
793
794 Mueller, A., Anselmetti, F., Ariztegui, D., Brenner, M., Hodell, D., Curtis, J., Escobar, J., Gilli,
795 A., Grzesik, D., Guilderson, T., Kutterolf, S., and Plötze, M.: Late Quaternary
796 palaeoenvironment of northern Guatemala: evidence from deep drill cores and seismic
797 stratigraphy of Lake Petén Itzá, *Sedimentology*, 57, 1220–1245, [10.1111/j.1365-3091.2009.01144.x](https://doi.org/10.1111/j.1365-3091.2009.01144.x), 2010.
798
799 Nogués-Bravo, D.: Predicting the past distribution of species climatic niches. *Glob. Ecol.*
800 *Biogeogr.*, 18, 521–31, <https://doi.org/10.1111/j.1466-8238.2009.00476.x>, 2009.
801



- 802 Nogués-Bravo, D., Rodríguez, J., Hortal, J., Batra, P., and Araújo, M.B.: Climate change,
803 humans, and the extinction of the woolly mammoth, *PLoS Biol.*, 6, e79,
804 <https://doi.org/10.1371/journal.pbio.0060079>, 2008.
- 805
- 806 Otto-Bliesner, B.L., Marshall, S.J., Overpeck, J.T., Miller, G.H., Hu, A., and CAPE Last
807 Interglacial Project members.: Simulating Arctic Climate Warmth and Icefield Retreat in the
808 Last Interglaciation, *Science*, 311, 1751–1753, <https://doi.org/10.1126/science.1120808>,
809 2006.
- 810
- 811 Pérez, L., Lorenschat, J., Brenner, M., Scharf, B., and Schwalb, A.: Extant freshwater
812 ostracodes (Crustacea: Ostracoda) from Lago Petén Itzá, Guatemala, *Rev. Biol. Trop.*, 58,
813 871–895, <https://doi.org/10.15517/rbt.v58i2.5252>, 2010.
- 814
- 815 Pérez, L., Frenzel, P., Brenner, M., Escobar, J., Hoelzmann, P., Scharf, B., and Schwalb, A.:
816 Late Quaternary (24–10 ka BP) environmental history of the Neotropical lowlands inferred
817 from ostracodes in sediments of Lago Petén Itzá, Guatemala, *J. Paleolimnol.*, 46, 59–74,
818 <https://doi.org/10.1007/s10933-011-9514-0>, 2011.
- 819
- 820 Perry, E., Velazquez-Oliman, G., and Marin, L.: The Hydrogeochemistry of the Karst Aquifer
821 System of the Northern Yucatan Peninsula, Mexico, *Int. Geol. Rev.*, 44, 191–221,
822 <https://doi.org/10.2747/0020-6814.44.3.191>, 2002.
- 823
- 824 Peterson, A.T., Martínez-Meyer, E., and González-Salazar, C.: Reconstructing the
825 Pleistocene geography of the *Aphelocoma jays* (Corvidae). *Divers. Distrib.*, 10, 237–246,
826 <https://doi.org/10.1111/j.1366-9516.2004.00097.x>, 2004.
- 827
- 828 Peterson, A.T., and Nyári, Á.: Ecological niche conservatism and Pleistocene refugia in the
829 thrush-like mourner, *Schiffornis* sp., in the Neotropics, *Evolution*, 62, 173–183,
830 <https://doi.org/10.1111/j.1558-5646.2007.00258.x>, 2008.
- 831
- 832 R Development Core Team., R: a language and environment for statistical computing. R
833 Foundation for Statistical Computing, Vienna. [www. r-project.org](http://www.r-project.org), 2015.
- 834
- 835 Ridgeway, G.: The state of boosting, *Computing Science and Statistics*, 31, 172–181, 1999.
- 836



- 837 Ruegg, K., Hijmans, R., and Moritz, C.: Climate change and the origin of migratory pathways
838 in the Swainson's thrush, *Catharus ustulatus*, *J. Biogeogr.*, 33, 1172–1182,
839 <https://doi.org/10.1111/j.1365-2699.2006.01517.x>, 2006.
- 840
- 841 Sandel, B., Arge, L., Dalsgaard, B., Davies, R.G., Gaston, K.J., Sutherland, W.J., and
842 Svenning, J.C.: The influence of Late Quaternary climate-change velocity on species
843 endemism, *Science*, 334, 660–664, <https://doi.org/10.1126/science.1210173>, 2011.
- 844 Schmitter-Soto, J., Comín, F., Escobar-Briones, E., Herrera, J., Alcocer, J., Suarez-Morales,
845 E., Elías-Gutiérrez, M., Díaz, V., Marin, L., and Steinich, B.: Hydrogeochemical and biological
846 characteristics of cenotes in the Yucatan Peninsula (SE Mexico). *Hydrobiologia*, 467, 215–
847 228, <https://doi.org/10.1023/A:1014923217206>, 2002.
- 848
- 849 Solomon, S., Bacci, M., Martins, J., Vinha, G., and Mueller, U.: Paleodistributions and
850 comparative molecular phylogeography of leafcutter ants (*Atta* spp.) provide new insight into
851 the origins of Amazonian diversity, *PLoS ONE*, 3, e2738,
852 <https://doi.org/10.1371/journal.pone.0002738>, 2008.
- 853
- 854 Thuiller, W., Lafourcade, B., Engler, R., and Araújo, M.B.: BIOMOD —a platform for
855 ensemble forecasting of species distributions, *Ecography*, 32, 369–373,
856 <https://doi.org/10.1111/j.1600-0587.2008.05742.x>, 2009.
- 857
- 858 Thuiller, W., Georges, D., and Engler, R.: Package 'biomod2': ensemble platform for species
859 distribution modeling. R package version 3,3–7, 2015.
- 860
- 861 Tsuruoka, Y.: A simple C++ library for maximum entropy classification. [http://www-](http://www-tsuji.is.s.u-tokyo.ac.jp/~tsuruoka/maxent/)
862 [tsuji.is.s.u-tokyo.ac.jp/~tsuruoka/maxent/](http://www-tsuji.is.s.u-tokyo.ac.jp/~tsuruoka/maxent/), 2006.
- 863
- 864 Van Bloem, S.J., Lugo, A.E., and Murphy, P.G.: Structural response of Caribbean dry forests
865 to hurricane winds: a case study from Guanica Forest, Puerto Rico, *J. Biogeogr.*, 33, 517–23
866 <https://doi.org/10.1111/j.1365-2699.2005.01450.x>, 2006.
- 867
- 868 Vázquez-Domínguez, E., and Arita, H.: The Yucatan peninsula: biogeographical history 65
869 million years in the making, *Ecology*, 33, 212–219, [https://doi.org/10.1111/j.1600-](https://doi.org/10.1111/j.1600-0587.2009.06293.x)
870 [0587.2009.06293.x](https://doi.org/10.1111/j.1600-0587.2009.06293.x), 2010.
- 871
- 872 Veloz, S.D., Williams, J.W., Blois, J.L., He, F., Otto-Bliesner, B., and Liu, Z.: No-analog
873 climates and shifting realized niches during the late quaternary: implications for 21st-century



874 predictions by species distribution models, *Glob. Change Biol.*, 18, 1698–713,
875 <https://doi.org/10.1111/j.1365-2486.2011.02635.x>, 2012.

876

877 Waltari, E., and Guralnick, R.: Ecological niche modelling of montane mammals in the Great
878 Basin, North America: examining past and present connectivity of species across basins and
879 ranges, *J. Biogeogr.*, 36, 148–161, <https://doi.org/10.1111/j.1365-2699.2008.01959.x>, 2009.

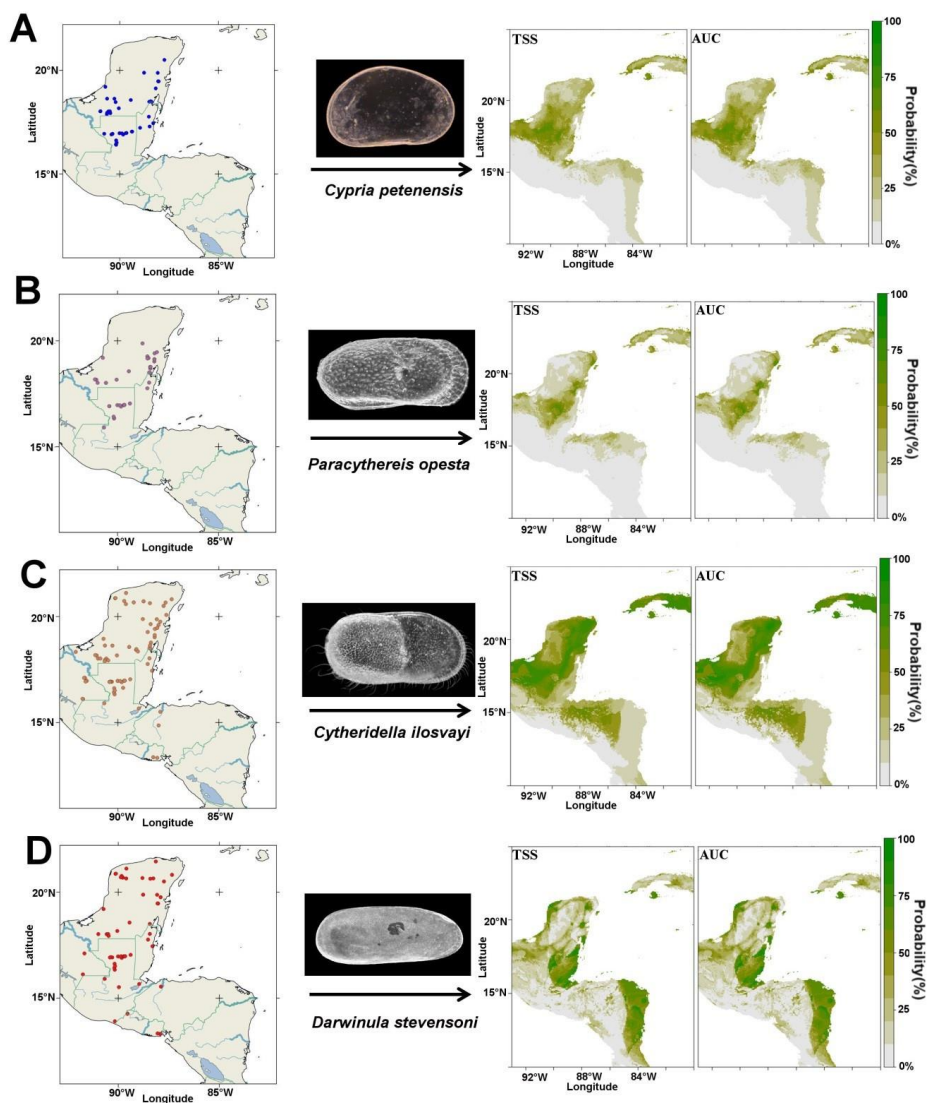
880

881 Watanabe, S., Hajima, T., Sudo, K., Nagashima, T., Takemura, T., Okajima, H., Nozawa, T.,
882 Kawase, H., Abe, M., Yokohata, T., Ise, T., Sato, H., Kato, E., Takata, K., Emori, S., and
883 Kawamiya, M.: MIROC-ESM 2010: model description and basic results of CMIP5-20c3m
884 experiments, *Geosci. Model Dev.*, 4, 845–872, <https://doi.org/10.5194/gmd-4-845-2011>, 2011.

885
886
887
888
889
890
891
892
893
894
895
896
897
898
899
900
901
902
903
904
905
906
907
908
909
910



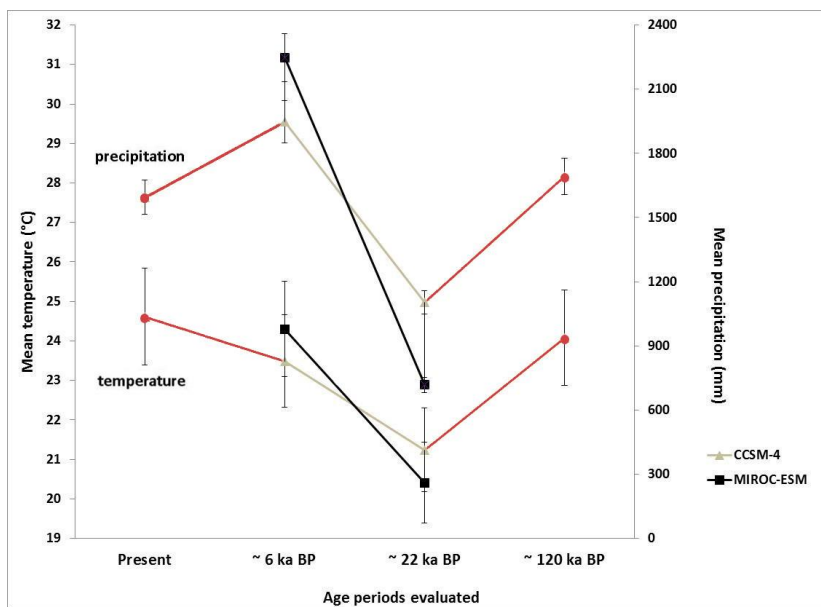
911 **Figures**



912

913 **Figure 1** Current ostracode species distributions and predicted distribution based on species
914 niche modeling and two statistical evaluations: true skill statistic (TSS) and area under the
915 receiver operating characteristic curve (AUC). A) *Cypria petenensis*, B) *Paracythereis*
916 *opesta*, C) *Cytheridella ilosvayi*, D) *Darwinula stevensoni*.

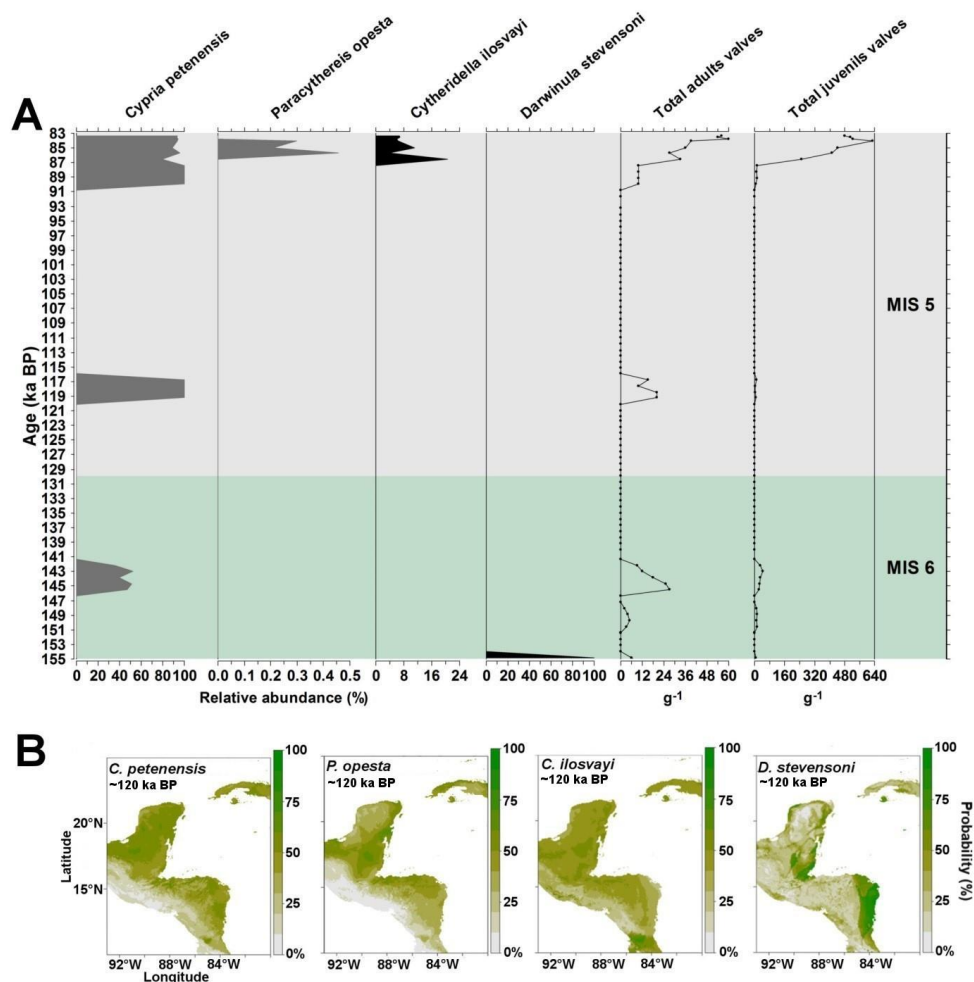
917



918

919 **Figure 2.** Estimated mean annual temperature and mean annual precipitation values for ~120
920 ka BP, ~22 ka BP, ~6 ka BP and present. Estimates for ~22 and ~6 ka BP were based on
921 general circulation models CCSM-4 (gray line) and MIROC-ESM (black line).

922



923

924

925 **Figure 3.** Fossil record of the period 155-83 ka BP and species niche modeling results for the
926 ~120 ka BP (representing Last Interglacial climate) for four ostracode species: *Cypria*
927 *petenensis*, *Paracythereis opesta*, *Cytheridella ilosvayi* and *Darwinula stevensoni*. A) Fossil
928 record of four ostracode species from core PI-1 in Lake Petén Itzá, and B) Maps from niche
929 modeling, showing the probability of species distributions.

930

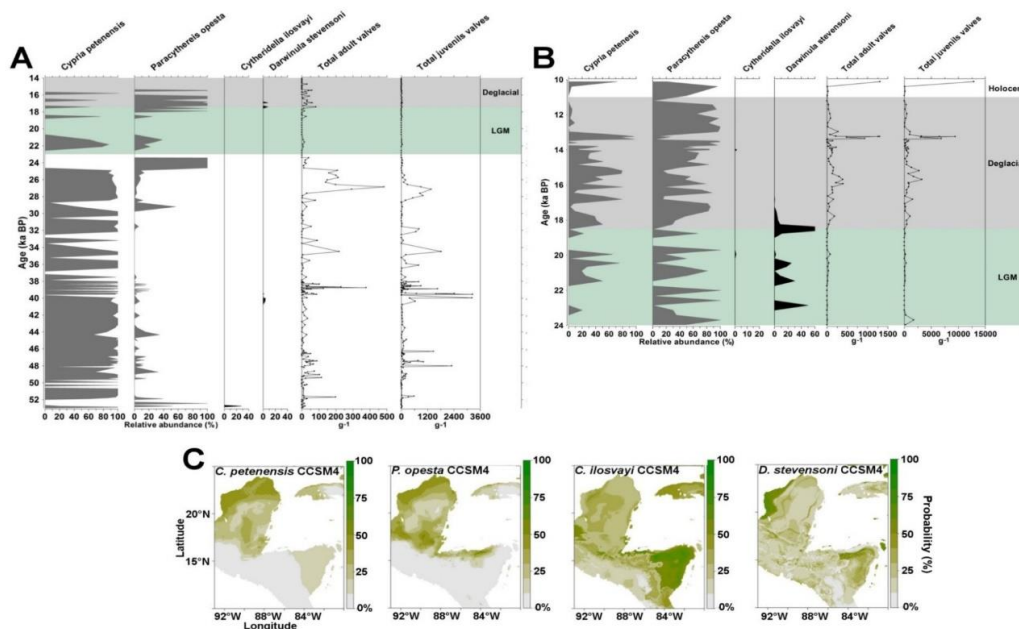


Figure 4. Fossil record of the period 53-10 and species niche modeling results for the ~22 ka BP (representing Last glacial maximum climate) for four ostracode species: *Cypria petenensis*, *Paracythereis opesta*, *Cytheridella ilosvayi* and *Darwinula stevensoni*. Fossil ostracode record from Lake Petén Itzá. A) Core PI-2 for the period 53-14 ka BP, B) Core PI-6 for the period 24-10 ka BP (taken from Pérez et al. 2011) and C) map showing the probability of species distributions based on the CCSM-4 climate model.

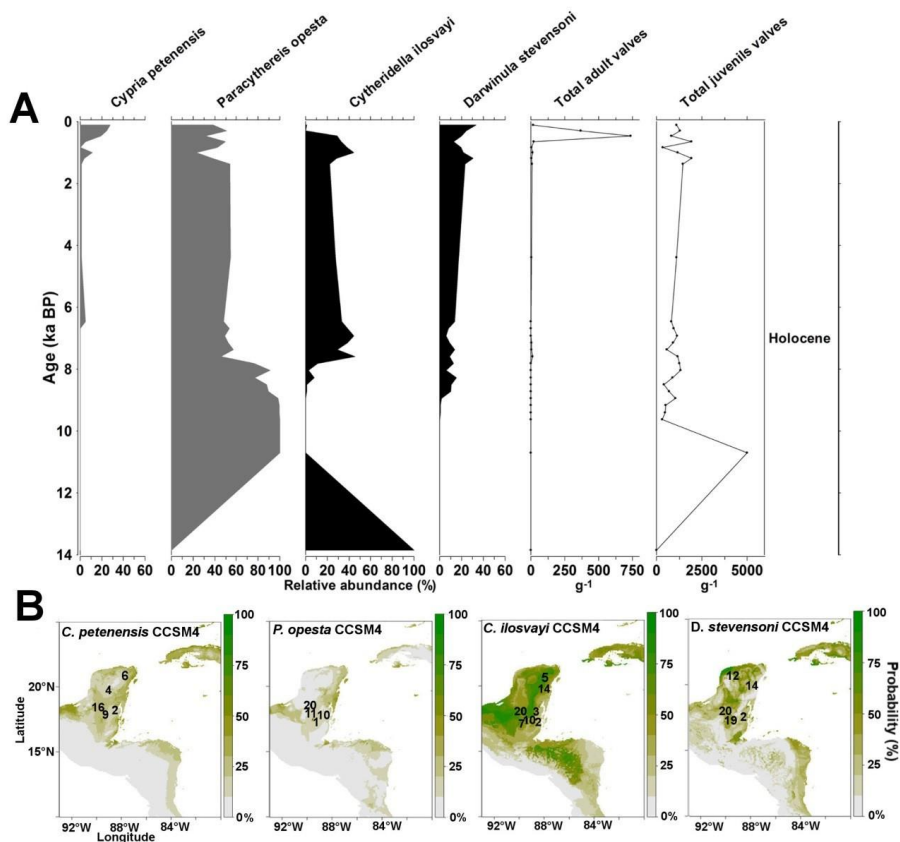


Figure 5. Fossil record of the last 14 ka and species niche modeling results for the ~6 ka BP (representing Mid-Holocene climate) for four ostracode species: *Cypria petenensis*, *Paracythereis opesta*, *Cytheridella ilosvayi* and *Darwinula stevensoni*. A) Ostracode fossil record from core Petén Itzá 22-VIII-99. B) Map showing the probability of suitable species distribution based on the CCSM-4 climate model. Numbers in maps represent regional fossil records. Numbers correspond to those in Supplementary material, Table S1.

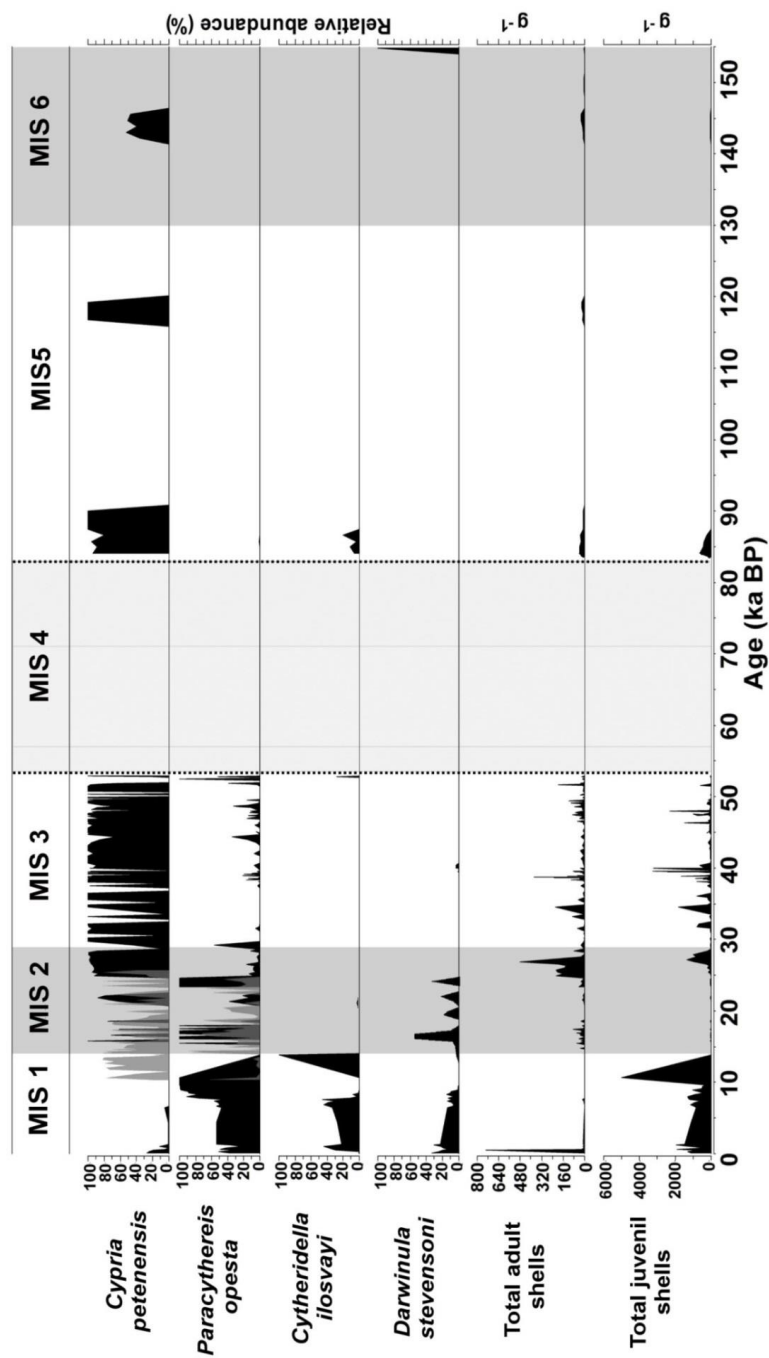


Figure 6. Master profile of the fossil ostracode record during Marine Isotope Stages of the last 155 ka in Lake Petén Itzá. Zone delimited by dashed lines represents a period of data absence. Gray peaks during the period of 24-10 represent results from core PI-6, whereas black peaks during the same period represent results from core PI-2.



1 **Table 1.** Ostracode species niche modeling, input data and evaluation scores. Variables of
 2 importance (mean of 10 evaluation runs) and evaluation model performances based on true
 3 skill statistic (TSS) and area under the receiver operating characteristic curve (AUC).
 4 Variable importance scores ≥ 0.30 are shown in bold.

5

Species	Presences	True absences	Variables importance	Evaluation of ensemble models		
				TSS	AUC	KAPPA
<i>Cytheridella ilosvayi</i>	79	112	BIO 1 (0.05), BIO 2 (0.03), BIO 3 (0.05), BIO 4 (0.46) , BIO 7 (0.13), BIO 12 (0.05), BIO 15 (0.30)	0.47	0.81	0.49
<i>Darwinula stevensoni</i>	61	130	BIO 1 (0.05), BIO 2 (0.39) , BIO 3 (0.01), BIO 4 (0.10), BIO 7 (0.01), BIO 12 (0.11), BIO 15 (0.11)	0.58	0.85	0.56
<i>Paracythereis opesta</i>	37	154	BIO 1 (0.10), BIO 2 (0.24), BIO 3 (0.10), BIO 4 (0.06), BIO 7 (0.14), BIO 12 (0.08) BIO 15 (0.48)	0.72	0.91	0.71
<i>Cypria petenensis</i>	49	142	BIO 1 (0.10), BIO 2 (0.30) , BIO 3 (0.09), BIO 4 (0.09), BIO 7 (0.15), BIO 12 (0.03), BIO 15 (0.31)	0.63	0.89	0.56

6

7

8